2017

Controlling the microstructure and associated magnetic properties of Ni0.2Mn3.2Ga0.6 melt-spun ribbons by annealing

Mahmud Khan
Miami University - Oxford, khanm2@miamioh.edu

Ohud Alshammari
Miami University - Oxford

Balamurugan Balamurugan
University of Nebraska-Lincoln, balamurugan@unl.edu

Bhaskar Das
University of Nebraska - Lincoln

David J. Sellmyer
University of Nebraska - Lincoln, dsellmyer@unl.edu

See next page for additional authors

Authors
Mahmud Khan, Ohud Alshammari, Balamurugan Balamurugan, Bhaskar Das, David J. Sellmyer, Ahmad Us Saleheen, and Shane Stadler

Controlling the microstructure and associated magnetic properties of $Ni_{0.2}Mn_{3.2}Ga_{0.6}$ melt-spun ribbons by annealing

Cite as: AIP Advances **7**, 056230 (2017); https://doi.org/10.1063/1.4977892
Submitted: 24 September 2016 . Accepted: 28 November 2016 . Published Online: 01 March 2017

Mahmud Khan, Ohud Alshammari, Balamurugan Balasubramanian, Bhaskar Das, David J. Sellmyer, Ahmad Us Saleheen, and Shane Stadler

AIP ADVANCES **7**, 056230 (2017)

Controlling the microstructure and associated magnetic properties of $Ni_{0.2}Mn_{3.2}Ga_{0.6}$ melt-spun ribbons by annealing

Mahmud Khan,[1,a] Ohud Alshammari,[1] Balamurugan Balasubramanian,[2] Bhaskar Das,[2] David J. Sellmyer,[2] Ahmad Us Saleheen,[3] and Shane Stadler[3]
[1]*Department of Physics, Miami University, Oxford, Ohio 45056, USA*
[2]*Department of Physics and Astronomy and Nebraska Center for Materials and Nanoscience, University of Nebraska, Lincoln, Nebraska 68588, USA*
[3]*Department of Physics and Astronomy, Louisiana State University, Baton rouge, Louisiana 70803, USA*

(Presented 1 November 2016; received 24 September 2016; accepted 28 November 2016; published online 1 March 2017)

Here we report on the structural and magnetic properties of $Ni_{0.2}Mn_{3.2}Ga_{0.6}$ melt-spun ribbons. The as-spun ribbons were found to exhibit mixed cubic phases that transform to non-cubic structure upon annealing. Additionally, an amorphous phase was found to co-exist in all ribbons. The SEM images show that minor grain formation occurs on the as-spun ribbons. However, the formation of extensive nano-grains was observed on the surfaces of the annealed ribbons. While the as-spun ribbons exhibit predominantly paramagnetic behavior, the ribbons annealed under various thermal conditions were found to be ferromagnetic with a Curie temperature of about 380 K. The ribbons annealed at 450 °C for 30 minutes exhibit a large coercive field of about 2500 Oe. The experimental results show that the microstructure and associated magnetic properties of the ribbons can be controlled by annealing techniques. The coercive fields and the shape of the magnetic hysteresis loops vary significantly with annealing conditions. Exchange bias effects have also been observed in the annealed ribbons. [http://dx.doi.org/10.1063/1.4977892]

INTRODUCTION

Permanent magnets based on neodymium-iron-boron (Nd-Fe-B) and other rare earth-based materials are the most powerful magnets, which are heavily applied in many technologies including compact electronic devices, motors for hybrid vehicles, and wind generators.[1,2] The increasing demand for rare-earth magnets has resulted in high cost and limited availability of rare-earth elements. Therefore, there is a growing interest in developing new magnetic materials that are free from the critical rare-earth elements. For permanent-magnet applications, the material of interest must exhibit large magnetocrystalline anisotropy (MCA).[3] Therefore, for the development of rare-earth-free magnets it is of great importance to develop ferromagnetic materials that exhibit large MCA.

Recently, some Mn-Ga based materials have gained intense research interest due to their large MCAs.[4–11] Depending on the stoichiometry and fabrication conditions, the structural and magnetic phases of these materials may vary dramatically.[4,5,12] From the perspective of permanent magnets, the tetragonal P4/mmm (ordered $L1_0$) and the I4/mmm (disordered $D0_{22}$) phases are of primary interest because they exhibit high Curie temperatures, large saturation, and large coercivity.[8,10,13] However, in order to fully exploit the permanent magnetic properties of these materials and make them suitable

[a]Corresponding author: Email: khanm2@miamioh.edu

for practical applications, they must be synthesized with desired composition and structure at the nanoscale level.

The desired nanostructures can be obtained by growing epitaxial thin-films,[5] ball-milling the materials into powders,[10] or by preparing melt-spun ribbons.[6,11] Considering the rare-earth-based permanent-magnet materials, it is well known that the microstructure and size of the nano-grains of the melt-spun ribbons can be controlled by optimizing the quenching rate as well as by annealing the rapidly-quenched ribbons under various conditions.[2,14,15] These methods have also been utilized to develop Mn-Ga based melt-spun ribbons.[6] In an attempt to further investigate the effectiveness of the melt-spinning method and annealing techniques in developing nanostructured Mn-Ga based hard magnetic materials, we have fabricated and characterized $Ni_{0.2}Mn_{3.2}Ga_{0.6}$ melt-spun ribbons. Our study shows that the hard magnetic properties of the rapidly-quenched ribbons are substantially improved by annealing.

EXPERIMENTAL TECHNIQUES

A polycrystalline button of $Ni_{0.2}Mn_{3.2}Ga_{0.6}$ weighing approximately 8 g was fabricated by arc-melting the constituent metals of more than 3N purity (obtained from Alfa Aesar, Inc.) in an argon atmosphere. The as-prepared button was then used for the preparation of the melt-spun ribbons. The ribbons were prepared using the melt spinning technique on a rotating copper wheel at a surface velocity of 57 ms^{-1}. The as-fabricated ribbons were then annealed at various temperatures for 30 minutes. The structure of the samples were verified by x-ray diffraction (XRD) measurements using a Scintag XDS 2000 that employed Cu Kα radiation with theta-theta geometry. The phase purities and microstructures of the alloys were analyzed by EDS in a Jeol JSM- 840A Scanning Electron Microscope (SEM). All XRD measurements were performed at room temperature. The magnetization measurements were carried out using a physical property measurement system (PPMS) from Quantum Design, Inc. The measurements were performed in the temperature range of 5 – 400 K and in applied

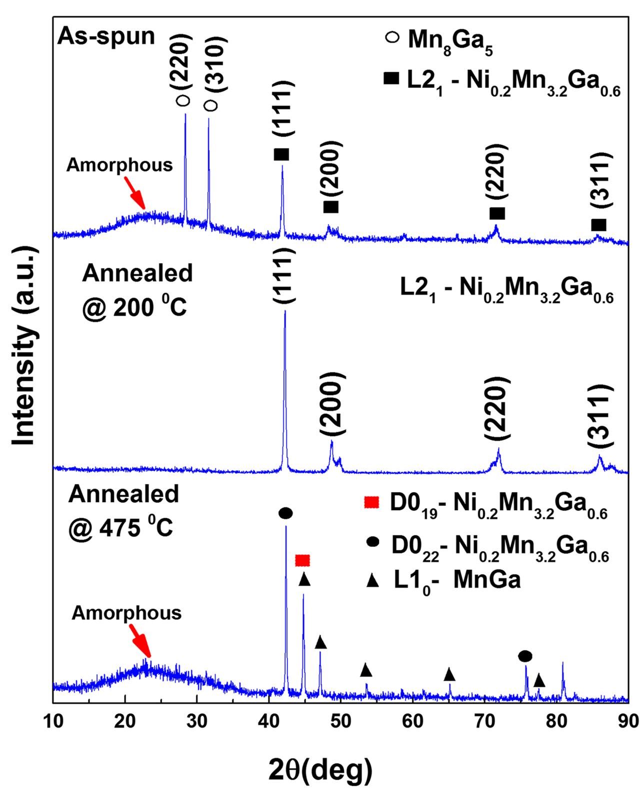

FIG. 1. Room temperature XRD patterns of selected $Ni_{0.2}Mn_{3.2}Ga_{0.6}$ ribbons annealed at various temperatures.

magnetic fields of up to 50 kOe. Before the zero-field-cooled (ZFC) measurements, the samples were cooled from room temperature to 5 K in zero magnetic field. The field cooled (FC) measurements were performed by cooling the samples in a magnetic field of 50 kOe.

RESULTS AND DISCUSSION

The XRD patterns of $Ni_{0.2}Mn_{3.2}Ga_{0.6}$ ribbons obtained at room temperature are shown in FIG. 1. The XRD patterns of the as-spun ribbons indicates that two major cubic phases co-existed in them. The primary phase was the $Ni_{0.2}Mn_{3.2}Ga_{0.6}$ cubic $L2_1$ phase and secondary phase was the cubic Mn_8Ga_5 phase, possibly with small amounts of Ni on the Mn sites. A noticeable change was observed in the XRD patterns of the ribbons annealed at 200 ^{0}C for 30 minutes. The (220) and (310) peaks corresponding to the Mn_8Ga_5 phase were not observed in those samples annealed at 200 ^{0}C. In addition, the peak near 42^0 (corresponding to the (111) $L2_1$ peak) was much sharper for these ribbons, suggesting that annealing at 200 ^{0}C promotes the formation of the $Ni_{0.2}Mn_{3.2}Ga_{0.6}$ cubic $L2_1$ structure. In the ribbons annealed at T > 450 ^{0}C, three distinct peaks were observed in the XRD data between 40^0 and 50^0, which could be indexed to a mixed phase primarily containing the $Ni_{0.2}Mn_{3.2}Ga_{0.6}$ DO_{22} and the hexagonal $Ni_{0.2}Mn_{3.2}Ga_{0.6}$ DO_{19} crystal structures, respectively.[16,17] Peaks corresponding to a small amount of the $L1_0$ MnGa phase were also observed in the data.

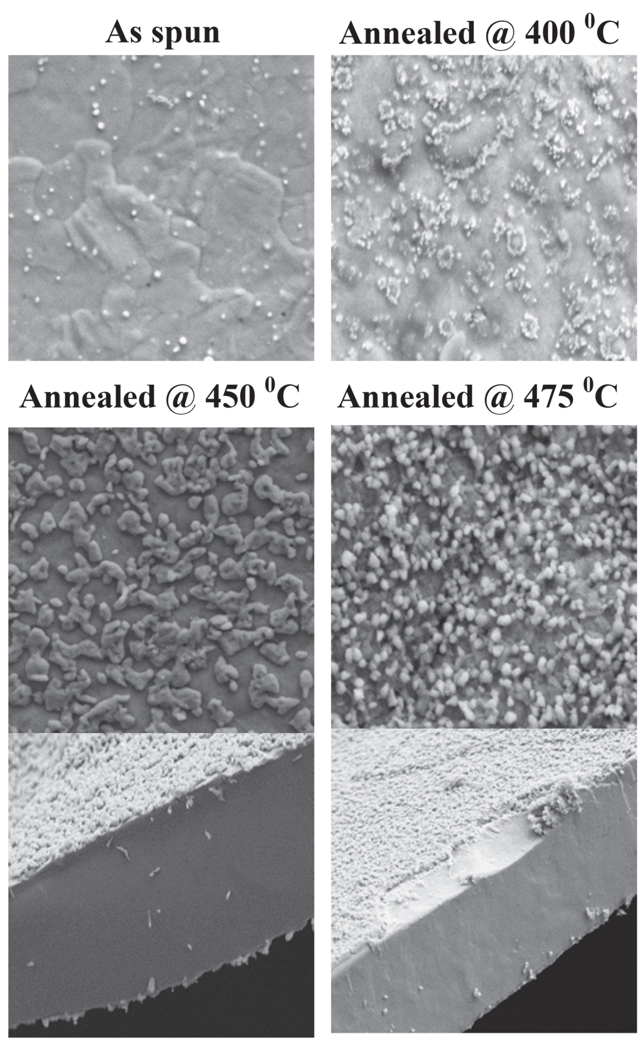

FIG. 2. Room temperature SEM micrographs of selected $Ni_{0.2}Mn_{3.2}Ga_{0.6}$ ribbons annealed at various temperatures.

As shown in FIG. 1, an amorphous phase, represented by the broad peak near 25^0 in the figure, was found to co-exist in all samples.

Figure 2 shows the SEM images of the as-spun $Ni_{0.2}Mn_{3.2}Ga_{0.6}$ ribbons and those annealed for 30 minutes at various temperatures. For the as-spun ribbons, grain formations at a significantly smaller scale were observed in the high resolution SEM micrographs. For the ribbons annealed at 400 ^{0}C, a minor grain growth was observed on the surface of the ribbons. A dramatic modification of the ribbon surfaces was observed when annealed at temperatures greater than 400 ^{0}C. A clear growth of nano-size grains was observed on the surfaces of the ribbons. Estimated from the SEM image, the grain sizes ranged between 50 - 70 nm. It is also interesting to note that the SEM micrographs of the cross-sections of the ribbons show that the nano-grains only grow on the surfaces of the melt-spun ribbons (not on the interiors). In addition, the cross-sectional SEM images show that there is no grain growth in the underlying matrix layer, which indicates its amorphous nature and is also supported by a broad hump observed around 25^0 in the x-ray diffraction patterns (Fig. 1). Thus, the sharp x-ray

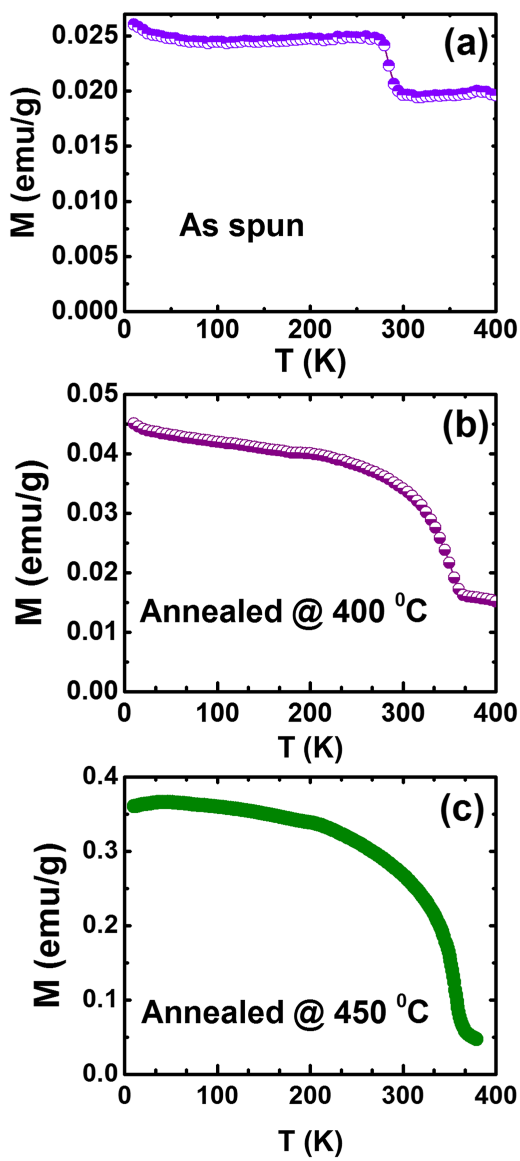

FIG. 3. Temperature dependence of the dc magnetization of selected $Ni_{0.2}Mn_{3.2}Ga_{0.6}$ ribbons measured in an applied magnetic field of 1 kOe.

diffraction patterns observed in Fig. 1 only represents the crystal structure of the nanograins. This behavior will be investigated further and the results will be reported elsewhere.

Figure 3 shows the magnetization as a function of temperature, *M* (T), for selected $Ni_{0.2}Mn_{3.2}Ga_{0.6}$ melt-spun ribbons. As shown in FIG. 3a, the magnetization of the as-spun ribbons remains nearly unchanged with increasing temperature until ~300 K, where it sharply drops but never reaches zero, even at 400 K. The unchanged *M* (T) curve with increasing temperature indicates that the sample is paramagnetic. The transition near 300 K may correspond to the Curie temperature of a weak and partially ordered $L2_1$ phase. The *M* (T) data of the ribbons annealed for 30 minutes at T = 400 ^{0}C and 450 ^{0}C are shown in Fig. 3b and 3c, respectively. The ribbons annealed at 400 ^{0}C exhibit a typical ferromagnetic behavior. Although the magnetization drops near T_c, it does not reach zero. The ferromagnetic nature is even more enhanced for the ribbons annealed at 450 ^{0}C. The Curie temperature is ~380 K for all ribbons annealed at temperatures > 400 ^{0}C.

The *M* (*H*) data measured at 5 K and 298 K for selected $Ni_{0.2}Mn_{3.2}Ga_{0.6}$ ribbons are shown in FIG. 4. For the as-spun ribbons (FIG. 4a), the *M* (H) data at both temperatures exhibit similar behavior, where the magnetization (which is significantly small) changes linearly with the applied magnetic field. The behavior suggests that as spun ribbons are non-ferromagnetic. As shown in Figure 4b, the hysteresis loops for the $Ni_{0.2}Mn_{3.2}Ga_{0.6}$ ribbons annealed at 400 °C for 30 minutes show a significant improvement. The hysteresis loop demonstrates hard magnetic behavior with a noticeable coercive field, which is higher at 5 K and much lower at 298 K. As the annealing temperature is increased (while keeping the annealing time constant at 30 minutes), the hard magnetic properties are significantly improved (see FIG. 4c and 4d). The coercive field at 5 K increases with increasing annealing temperature from 1665 Oe (400 ^{0}C) to 2528 Oe (450 ^{0}C) and then decreases to 1829 Oe (475 ^{0}C). The coercive field finally decreases to 1731 Oe when annealed at 500 °C (not shown here). It should be noted that, although the annealed ribbons exhibit enhanced coercivity, the magnetizations for all ribbons are significantly small. The reason for this behavior can be attributed to the fact that the nano grains only develop on the surfaces of the melt-spun ribbons as mentioned earlier.

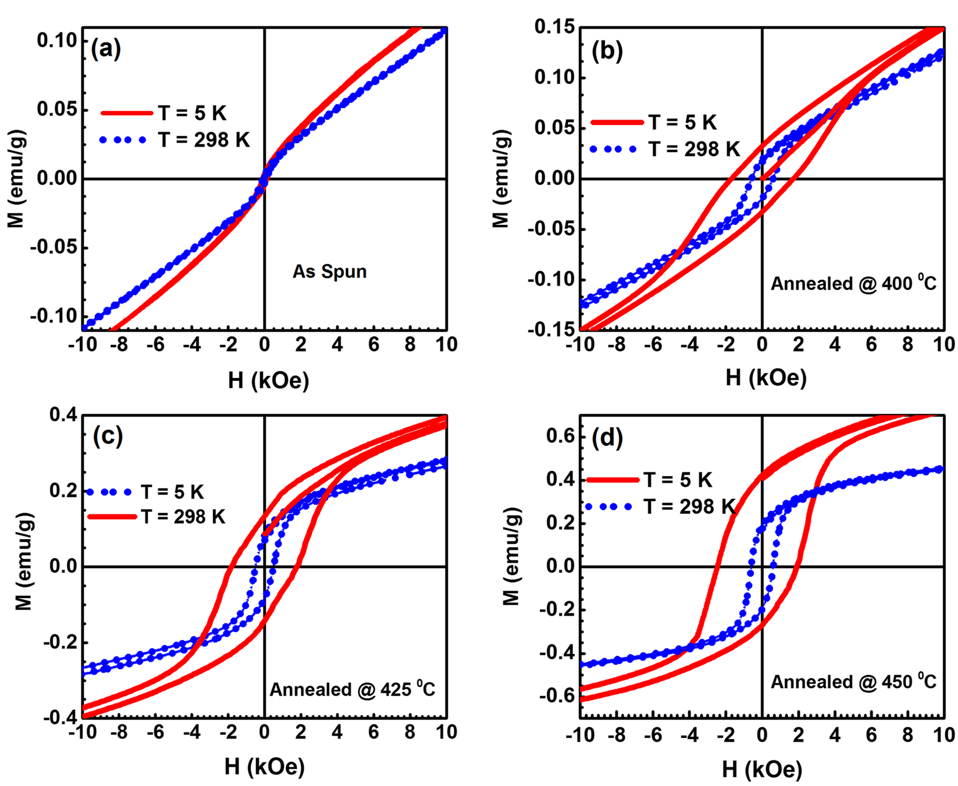

FIG. 4. Field dependence of the magnetization of $Ni_{0.2}Mn_{3.2}Ga_{0.6}$ ribbons measured at 5 K and 298 K.

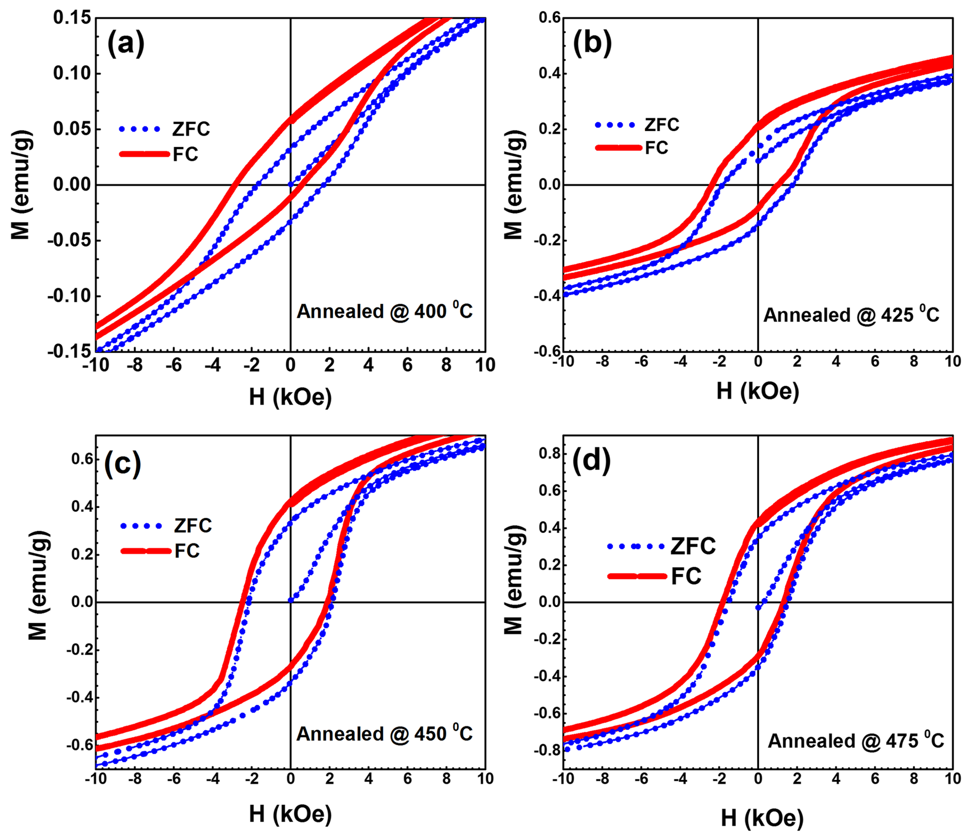

FIG. 5. Field dependence of the magnetization of $Ni_{0.2}Mn_{3.2}Ga_{0.6}$ ribbons measured at 5 K under ZFC and FC conditions.

The $M(H)$ data obtained under ZFC and FC conditions revealed additional characteristics of the $Ni_{0.2}Mn_{3.2}Ga_{0.6}$ ribbons, as shown in FIG. 5. Shifts in the hysteresis loops were observed when the samples were cooled from room temperature to 5 K in the presence of a magnetic field of 50 kOe. This behavior shows that the samples exhibit exchange bias, which signifies the co-existence of $D0_{19}$ antiferromagnetic and $L1_0$ / $D0_{22}$ ferromagnetic/ferromagnetic phases in the ribbons.[17] With increasing annealing temperature, the magnitude of the exchange bias is reduced, suggesting a reduction in the antiferromagnetic phases with increasing annealing temperature.

The experimental results presented above confirm that by controlling the annealing conditions, the microstructure and the associated hard magnetic properties of $Ni_{0.2}Mn_{3.2}Ga_{0.6}$ melt-spun ribbons can be manipulated. Further optimization is necessary for complete formation of nano-grains throughout the entire ribbons (instead of just on the surfaces). Considering that such grain formation occurs, the net magnetization and coercivity of the ribbons are expected to increase significantly. Additionally, for the determination of the exact elemental compositions of the nano-grains that formed on the ribbons, more measurements, including TEM, will need to be performed on them.

CONCLUSION

In conclusion, we have investigated the structural and magnetic properties of $Ni_{0.2}Mn_{3.2}Ga_{0.6}$ melt-spun ribbons. The as-spun ribbons were found to exhibit mixed cubic phases while the annealed ribbons exhibited tetragonal structures. Annealing the ribbons resulted in the formation of nano-size grains on the surfaces. The annealed ribbons showed ferromagnetic behavior with a Curie temperature of 380 K. The largest coercive field of 2528 Oe was observed for the ribbons annealed at 450 ^{0}C for 30 minutes. The observation of exchange bias in the ribbons demonstrates the coexistence of antiferromagnetic and ferromagnetic (and or ferrimagnetic) exchange interactions. The observed experimental results indicate that the Ni-Mn-Ga based materials should be investigated further for the development of rare-earth-free permanent magnets.

ACKNOWLEDGMENTS

The SEM micrographs and the related EDS data were obtained by Matthew L. Duley at the center of advanced microscopy and imaging (CAMI) of Miami University. Shane Stadler (LSU) was supported by the Office of Basic Energy Sciences, Materials Science Division of the U.S. Department of Energy, DOE Grant No. DE-FG02-13ER46946. Research at Nebraska was supported by the U.S. Department of Energy (Grant No. DE-FG02-04ER46152) and was performed in part in the Nebraska Nanoscale Facility: National Nanotechnology Coordinated Infrastructure and the Nebraska Center for Materials and Nanoscience, which are supported by the National Science Foundation under Award ECCS: 1542182, and the Nebraska Research Initiative.

[1] S. Sugimoto, "Current status and recent topics of rare-earth permanent magnets," J. Phys. D: Appl. Phys. **44**, 064001 (2011).
[2] A. K. Pathak, M. Khan, K. A. Gschneidner, Jr., R. W. McCallum, L. Zhou, K. Sun, K. W. Dennis, C. Zhou, F. E. Pinkerton, M. J. Kramer, and V. K. Pecharsky, Adv. Mater **27**, 2663 (2015).
[3] B. D. Cullity and C. D. Graham, *Introduction to Magnetic Materials* (John Wiley & Sons, Inc., Hoboken, New Jersey, 2009), p. 220.
[4] H. Niida, T. Hori, H. Onodera, Y. Yamaguchi, and Y. Nakagawa, J. Appl. Phys. **79**, 5946 (1996).
[5] T. J. Nummy, S. P. Bennett, T. Cardinal, and D. Heiman, "Large coercivity in nanostructured rare-earth-free Mn_xGa films," Appl. Phys. Lett. **99**, 252506 (2011).
[6] T. Saito and R. Nishimura, J. Appl. Phys. **112**, 083901 (2012).
[7] T. Saito and D. Nishio-Hamane, AIP Advances **6**, 075004 (2016).
[8] Q. M. Lu, M. Yue, H. G. Zhang, M. Wang, F. Yu, Q. Huang, D. H. Ryan, and Z. Altounian, Scientific Reports **5**, 17086 (2015).
[9] M. E. Jamer, B. A. Assaf, S. P. Bennett, L. H. Lewis, and D. Heiman, "Magnetic properties and large coercivity of MnxGa nanostructures," J. Magn. Magn. Mater **358-359**, 259 (2014).
[10] A. A. El-Gendy and G. Hadjipanayis, "Nanostructured $D0_{22}$-Mn_3Ga with high coercivity," J. Phys. D: Appl. Phys. **48**, 125001 (2015).
[11] Y. Huh, P. Kharel, V. R. Shah, X. Z. Li, R. Skomski, and D. J. Sellmyer, J. Appl. Phys. **114**, 013906 (2013).
[12] J. Winterlik, B. Balke, G. H. Fecher, C. Felser, M. C. M. Alves, F. Bernardi, and J. Morais, Phys. Rev. B **77**, 054406 (2008).
[13] L. J. Zhu, S. H. Nie, K. K. Meng, D. Pan, J. H. Zhao, and H. Z. Zheng, Adv. Mater **24**, 4547 (2012).
[14] J. J. Croat, J. F. Herbst, R. W. Ree, and F. E. Pinkerton, J. Appl. Phys. **55**, 2078 (1984).
[15] J. Wecker and L. Schultz, J. Appl. Phys. **62**, 990 (1987).
[16] W. Gong, X. Zhao, W. Fan, J. Feng, A. Lin, J. He, W. Liu, and Z. Zhang, IEEE Trans. Magn. **51**, 2101104 (2015).
[17] J. N. Feng, X. G. Zhao, X. K. Ning, C. W. Shih, W. C. Chang, S. Ma, W. Liu, and Z. D. Zhang, J. Appl. Phys. **115**, 17A750 (2014).